Journal of Materials and Environmental Sciences
ISSN : 2028-2508
CODEN : JMESCN

J. Mater. Environ. Sci., 2020, Volume 11, Issue 1, Page 8-14

http://www.jmaterenvironsci.comm

Study of Al-Doped and Al/N Co-Doped TiO_2 Nanoparticles for Dye Sensitized Solar Cells

S. Saravanan[1], R.S. Dubey[1]

[1]*Advanced Research Laboratory for Nanomaterials & Devices, Department of Nanotechnology, Swarnandhra College of Engineering & Technology, Seetharampuram, Narsapur- 534 280, West Godavari (A.P.), India*

Received 12 July 2019,
Revised 21 Nov 2019,
Accepted 22 Nov 2019

Keywords
- ✓ Sol-gel,
- ✓ Nanoparticles,
- ✓ Photoanode,
- ✓ DSSC,
- ✓ Photovoltaic.

shasa86@gmail.com ;
Phone: +08814240588

Abstract

Sol-gel synthesis of aluminium (Al)-doped TiO_2 (ALT) and aluminium/nitrogen (Al/N) co-doped TiO_2 (ALNT) nanoparticles were carriedout. The various investigations were done to examine the crystallinity, vibrational modes of elements presented in the samples, surface morphology and composition elementals using X-ray diffractometer (XRD), Raman spectroscopy, field emission scanning electron microscopy (FESEM) and energy dispersive spectroscopy (EDS) respectively. XRD study stated the good crystallinity of ALT particles as compare ALNT particles and no other peaks are noticed other than anatase phase in the both the samples. As a result of doping, the Raman peak is found to be shifted towards the higher wavenumber for the case of both the samples. FESEM analysis showed the spherical shape morphological of ALT and ALNT NPs. The average diameters of the NPs are 14 and 9 nm corresponding to the ALT and ALNT samples. The elemental composition peaks of aluminium (Al), titanium (Ti), nitrogen (N) and oxygen (O_2) peaks were noticed by EDS measurements. Furthermore, both the prepared nanoparticles were used as the photoanode materials in the dye-sensitized solar cells (DSSCs) where as ALT based materials showed the enhanced photovoltaic (PV) performance.

1. Introduction

The third-generation solar cells, particularly dye sensitized solar cells (DSSCs) are known to be promising renewable energy sources due to their low-cost, easy fabrication process and even it is possible to fabricate on flexible substrates [1-3]. DSSC is integrated with the dye anchored nanocrystalline-TiO_2 semiconductor layer on to fluorine-doped tin oxide (FTO) glass as the photo-anode, platinum (Pt) or carbon-coated FTO as the counter electrode and the electrolyte in-between these two plates. Among these parts, photo-anode plays a crucial role due to their photo-generation and dye-absorption which affects the current-density (Jsc) and the power conversion cell efficiency (Ƞ). TiO_2 is the most prominent semiconductor metal oxide material for the DSSCs and the photocatalytic applications [4]. As of now, the maximum reported DSSC efficiency is 14.3% by employing mesoporous TiO_2 layer [5]. Owing to wide energy bandgap 3.2 eV of the TiO_2 it uses the small fraction <5% of the solar spectrum. Therefore, the ongoing research is focusing to improve the optical properties of the TiO_2. Many reports have been reported on the synthesis of TiO_2 nanoparticles (NPs) using sol-gel, solvothermal, hydrothermal, electrospinning etc. However, by doping the optical bandgap of the TiO_2 can be modified. Generally, the integration of metal (Ag, Cu, Al and W), non-metal (B, N and C), metal non-metal (Zr/N, Mo/C and Al/N) co-doping TiO_2 nanostructure harvesting the improved performance in DSSCs. Jose et al. reported the binary and ternary doped TiO_2 nanoparticles as the photoanode materials of the DSSCs. The doping of Nb_2O_5 and Nb in TiO_2 showed better crystallinity and the high performance of the DSSCs [6]. *Jin et al.* prepared the crystalline anatase-TiO_2 nanoparticles and used as the photoelectrode material for the DSSCs. The parameters like open-circuit voltage (V_{OC}), the rate of electron transfer and the different doping concentration of Al and Zn were studied. The photovoltaic conversion efficiency of pure-TiO_2, Al-doped TiO_2 and Zn-doped TiO_2 were 3.9, 5.86 and 5.58%

respectively. Further, the enhanced photovoltaic efficiency 7.12% with the current density 14.38 mA/cm^2 were obtained using Al and Zn co-doped TiO_2 nanoparticles [7]. *Wu et al.* demonstrated the improved short-circuit current by using Zn-doped TiO_2 as the electron transfer layer. The zinc-doped TiO_2 layer was prepared via the sol-gel process by varying the doping concentration. Finally, the perovskite solar cells by optimizing the process parameters showed the enhanced current density 22.3 mA/cm^2 and power conversion efficiency 14.0% [8]. *Li et al.* deposited the Al-doped TiO_2 layer on mesoporous TiO_2 film by using chemical bath deposition (CBD) process with the goal to enhance the power conversion efficiency of the DSSCs. They observed the improved electron mobility and suppressed charge-carrier recombination as a result, the conversion efficiency was improved as much as 7.66% [9]. *Govindaraj et al.* synthesized the mesoporous anatase TiO_2 nanoparticles using the sol-gel process and the XRD pattern showed the anatase-TiO_2 crystalline nature while UV-Vis DRS spectrum evidenced the absorption in the UV region. The DSSCs prepared using these nanoparticles showed as much as 3.415 % conversion efficiency and 13.2 mA/cm^2 short-circuit current density [10].

In the presented work, the sol-gel synthesis of ALT and ALNT nanoparticles and studied the structural, morphological performance. The source materials and experimental procedures are presented in section 2. The properties of prepared doped and co-doped TiO_2 nanoparticles are discussed in section 3. Finally, concluded in section 4.

2. Material and Methods

2.1. Chemicals

Titanium tetra isopropoxide ($C_{12}H_{28}O_4Ti$), aluminum nitrate nonahydrate ($Al(NO_3)_3.9H_2O$), de-ionized water (DI), methanol (CH_3OH), isopropyl alcohol (C_3H_8O), titanium tetrachloride ($TiCl_4$) and carbamide (CH_4N_2O), glacial acetic acid (CH_3COOH), hydrochloric acid (HCl) and polyethylene glycol ($C_{2n}H_{4n+2}O_{n+1}$) were used as procured without any purification.

2.2. Synthesis Process

ALT nanoparticles were synthesized using the sol-gel technique and the procedural steps are illustrated in figure 1(a). First, 0.17 g aluminium nitrate nonahydrate was mixed with 15 ml DI water and later, 1.25 ml glacial acetic acid was added to form a uniform 'solution A'. Next, the 'solution B' was prepared by mixing 3.5 ml TTIP in 10 ml methanol which was stirred for 5 minutes. Under the stirring condition, the 'solution B' added into the 'solution A' by drop-wise and maintained the constant intervals. This final solution was stirred for 120 minutes and later, kept for aging at room temperature for 24 hrs. After the aging, the solution was dried at 80℃ for 15 hrs. Finally, the prepared sample was grinded and calcined at 450℃ for 2 hours. Similarly, ALNT nanoparticles were prepared by the sol-gel method as depicted in figure 1 (b). Initially, the 'solution C' was prepared by dissolving in 3.5 ml titanium tetra isopropoxide (TTIP) in 10 ml isopropyl alcohol (IPA) under stirring for 30 minutes at temperature 60℃. Next, the 'solution D' was prepared with 3 g aluminium nitrate nonahydrate and 2.96 g carbamide by dissolving in 100 ml DI water. The solutions 'C' and 'D' were mixed gradually and stirred for 30 minutes at room temperature. Further, hydrochloric acid (HCl) was added to maintain the pH to 4. The prepared homogeneous solution was dried in hot air-oven at 80℃ for 19 hours and finally, grinded powder was calcined a 460℃ for 90 minutes.

2.3 Preparation of Photoanodes and DSSCs

The prepared sample of Al-doped TiO_2 and Al/N co-doped TiO_2 nanoparticles were named as ALT and ALNT. The ALT and ALNT pastes were prepared separately by mixing in ethyl cellulose and acetic acid which were further grinded. The mixed solution was kept in a hot air oven at 100℃ for few minutes in order to remove the excess solution and to get the slurry paste. Before the photoanode preparation, substrates were cleaned individually with acetone and DI water in a sonicator bath for 10 minutes. Next, all the samples dipped in 40 mM $TiCl_4$ for 24 hrs at 40℃ and later, the FTO substrates were rinsed in DI water to remove the excess $TiCl_4$. After washing, the FTO substrates were dried for 30 minutes at 100℃ and finally coated the paste of ALT and ALNT were rolled on the FTO plates by doctor blade method. All the photoanodes were dried at 70℃ for 10 minutes and calcined at

460°C for 60 minutes. Finally, the photoanodes were immersed in ruthenium dye for 24 hrs. Later, we used to assemble DSSCs after rinsing in DI water in order to remove the excess of dye-loading. For DSSC fabrication, the dye adsorbed photoanodes and platinum (Pt) counter electrodes were integrated face to face by keeping a Surlyn film in between. Further, an electrode solution containing potassium iodide (KI) was filled between the photoanode and the counter electrode. For the packing purpose, the paper binder clips were used.

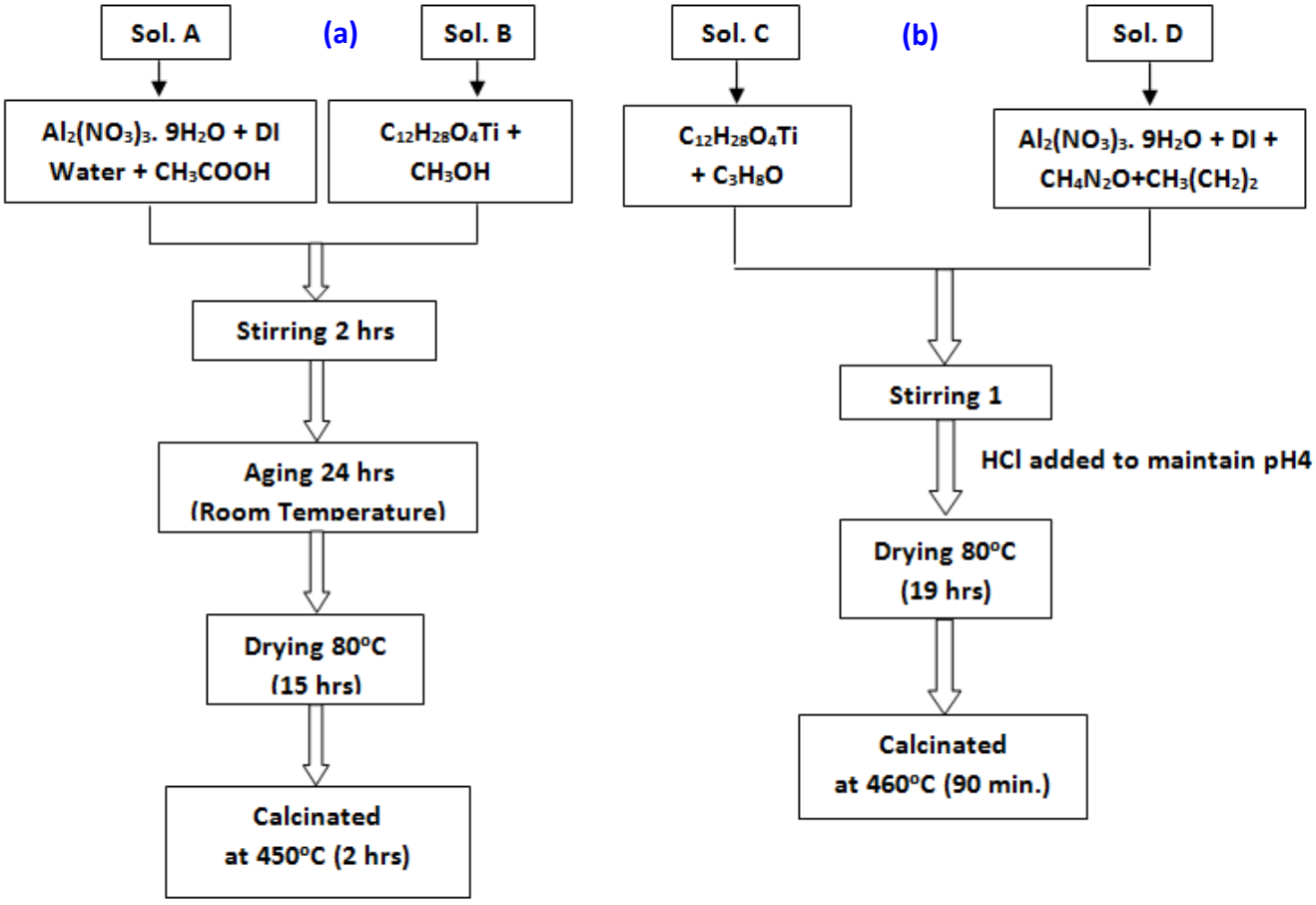

Figure 1: The sol-gel process for the preparation of ALT (a) and ALNT nanoparticles.

After the calcination, the prepared nanoparticle properties were characterized by X-ray diffractometer (Bruker D8, Venture), Micro Raman Spectrometer, scanning electron microscopy (FEI-Nove NanoSEM 450), energy-dispersive X-ray spectroscopy (Bruker- XFlash 6130) respectively.

3. Results and discussion

The synthesized nanoparticles were characterized by powder X-ray diffractometer (XRD) to study their crystalline phase. Figure 2(a) and (b) shows the XRD patterns of ALT and ALNT samples prepared by the sol-gel method. These patterns depict the anatase-TiO_2 phase present in both the samples without any other impurities or phases (rutile or brookite). The anatase phases are retained after the ALT and ALNT. The peaks representing the anatase phase at 2θ= 25.4°, 38°, 48.1°, 54.1°, 54.9°, 62.86°, 68.92°, 70.14° and 75.26° is noticed in ALT sample. The high intensity of the plane peak (101) indicates good crystallinity of the polycrystalline nanoparticles [11]. Similarly, XRD pattern of the ALNT nanopowder showed the Bragg's peaks at 2θ= 25.2°, 37.9°, 48.05°, 54.67°, 62.58°, 69.7° and 75.71° corresponding to the planes (101), (004), (200), (211), (204), (116) and (215). As compared to ALNT sample, the ALT showed the sharp peaks for example (101) peaks as depicted in the inset figure 2. The shifting of diffraction peaks towards the lower angle can also be noticed for the sample ALNT and our result is consistent with the reported one [12-13]. The broadening of diffraction peak corresponds to the smaller crystallite size. *Gurkan et al.* explained the broadening of the diffraction peak associated to represents the reduction in the small crystallite size and high disorder of the particles [14].

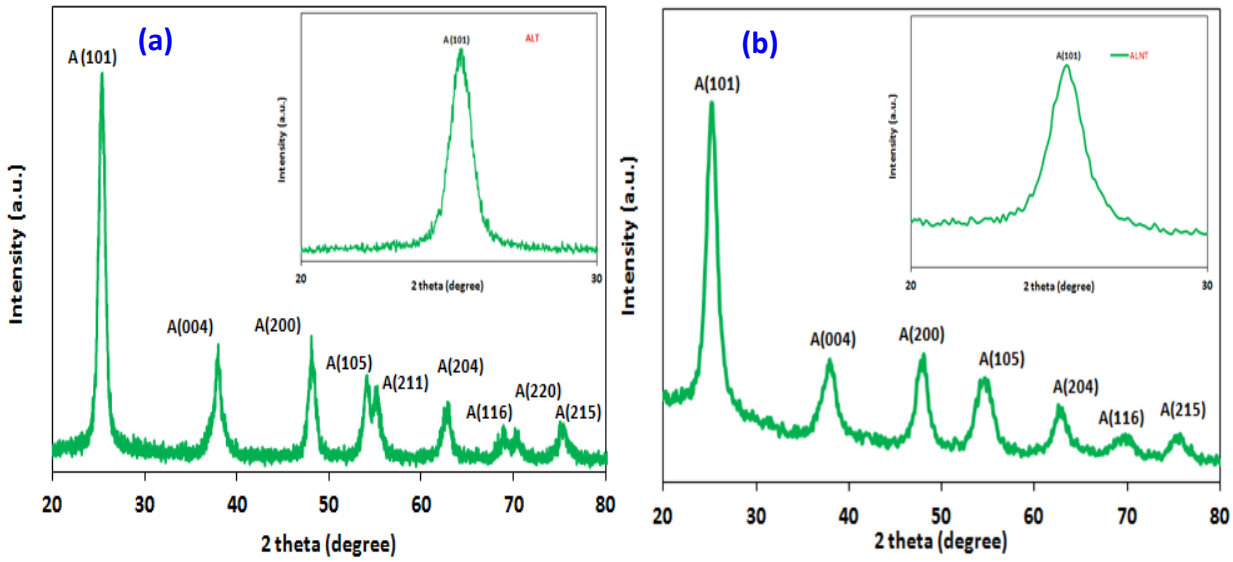

Figure 2. XRD pattern of ALT (a) and ALNT (b) nanopowders.

Raman spectroscopy is a powerful tool to study the structural and surface stoichiometric information of inorganic oxides like TiO_2. Figure 3(a) and 3(b) shows the Raman spectra of ALT and ALNT samples. The undoped anatase-TiO_2 shows five vibrational modes at 140/147, 188/197, 388/396, 507/514 and 631/636 cm^{-1} corresponding to 1Ag+2B1g+3Eg modes as reported in the literature [15-16]. Figure 3(a) shows the four significant peaks corresponding to the vibrational modes of anatase-TiO_2 phase as Eg (145cm^{-1}), B1g (397 cm^{-1}), A1g/B1g (516 cm^{-1}) and Eg (639 cm^{-1}) [14, 15]. From the reported works, these vibrational peaks are slightly shifted towards higher wave number due to Al doping which confirmed the doping of Al^{3+} ions in O-Ti-O lattice. Similarly, figure 3(b) depicts the Raman spectra of ALNT sample while the main peak position is found to be shifted to 153 cm^{-1}. This could be due to the presence of N^{3-} ions which modified the normal vibration modes of the TiO_2 after the doping. The main peak (peak) is also depicted in the inset of figure 3. For the case of ALNT sample, a wider peak endorses the oxygen (O_2) defect [15]. The changes in the Raman spectra are related to the substitutional doping of nitrogen with the reason of various ionic radii, oxidation states, electro-negativity etc. while the oxygen vacancy strongly affects the Raman shift as shown in figure 3 (b) [17].

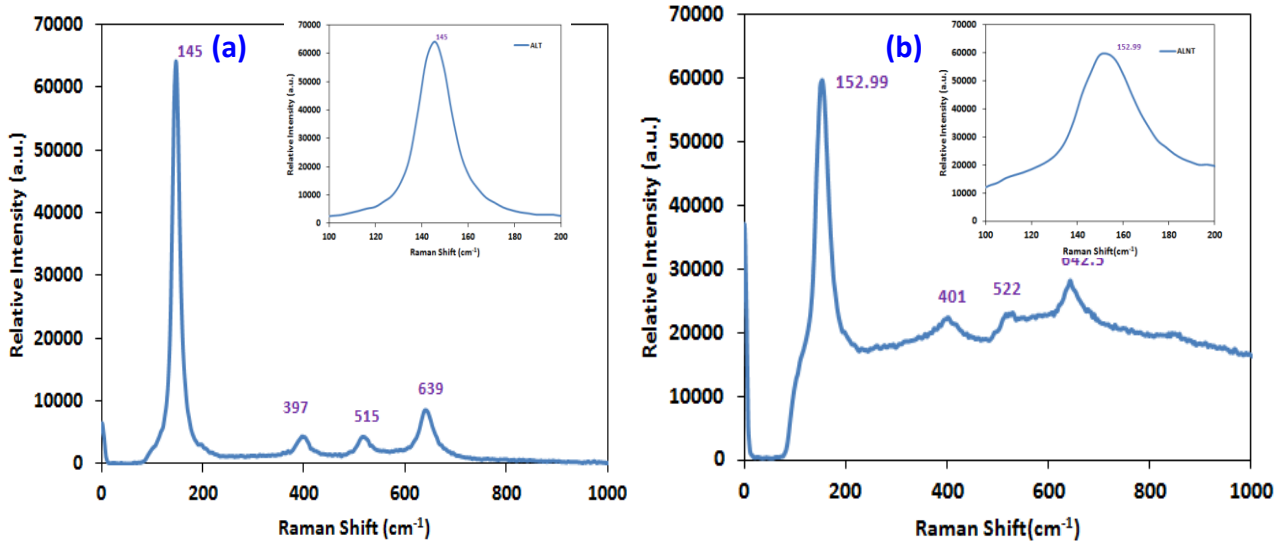

Figure 3. Raman spectra of ALT (a) and ALNT (b) nanoparticles.

Figure 4 depicts the FESEM images of the ALT and ALNT nanoparticles. Figure 4(a) shows the preparation shape spherical shaped nanoparticles with their diameter from 12-16 nm. Similarly, figure 4(b) evidences the spherical

shape nanoparticles with agglomerated. However, the estimated size was in the range from 7-12 nm. From the XRD studies, confirmed the properties of crystallinity and size reductant behaviour due to 'N' co-doping. Figure 4 (c-d) depicted the EDS spectrum of the synthesized ALT and ALNT nanoparticles. The presence of aluminium, titanium and oxygen is evidenced in figure 4 (c). In the same way, ALNT sample confirmed the elemental peaks of aluminium, oxygen, nitrogen and titanium as depicted in figure 4(d).

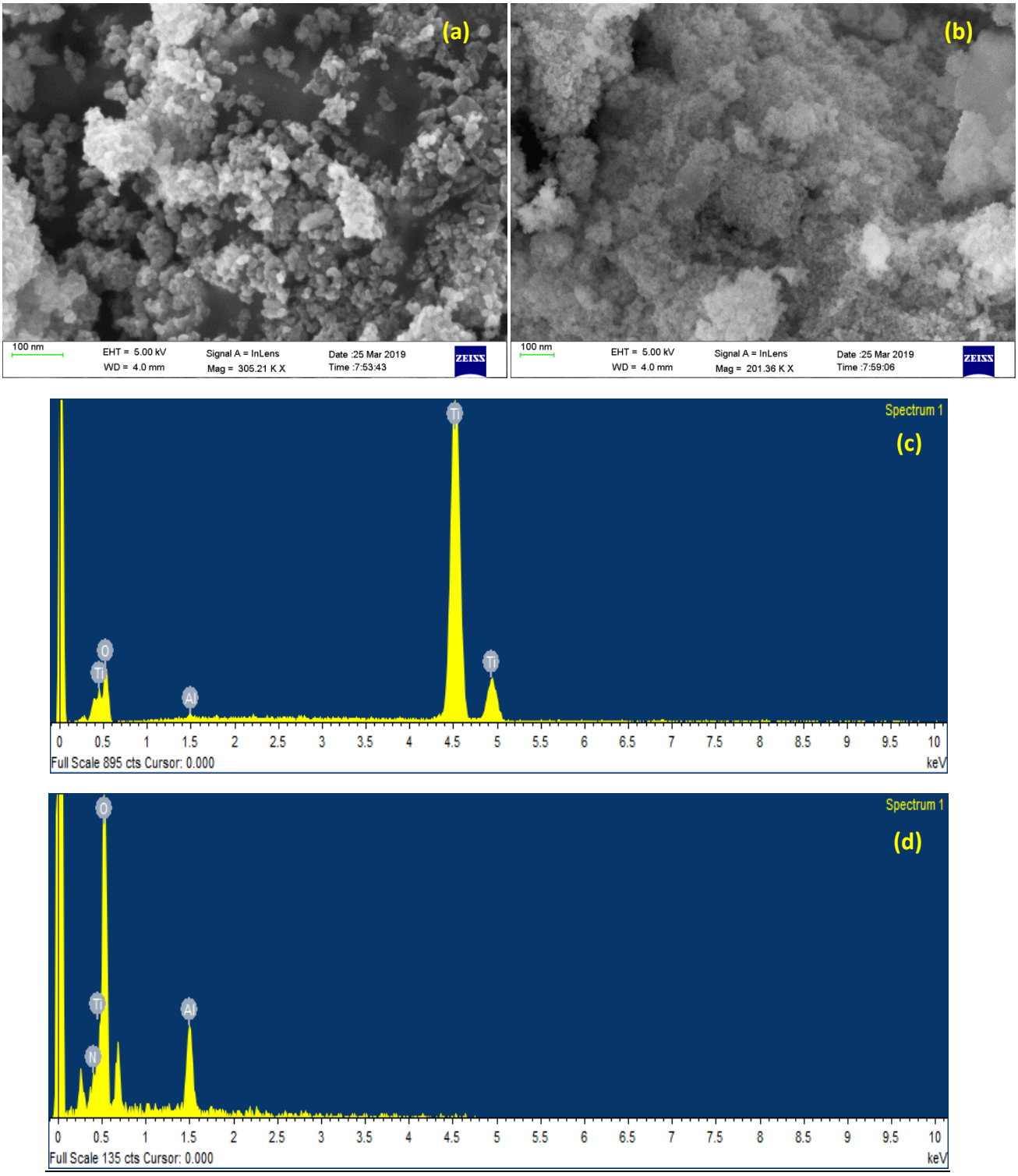

Figure 4. FESEM images of ALT (a), ALNT (b) and EDS spectrum of ALT (c) and ALNT (b) nanoparticles

Figure 5 shows the J-V curve of the DSSCs based on the ALT and ALNT photoanodes. Significant enhancements in the current density of 5.42 mA/cm^2 and cell efficiency (Ƞ) 1.48% were achieved by using the photoanode based on ALT nanoparticles due to the high surface area, higher dye absorption, stability etc [12].

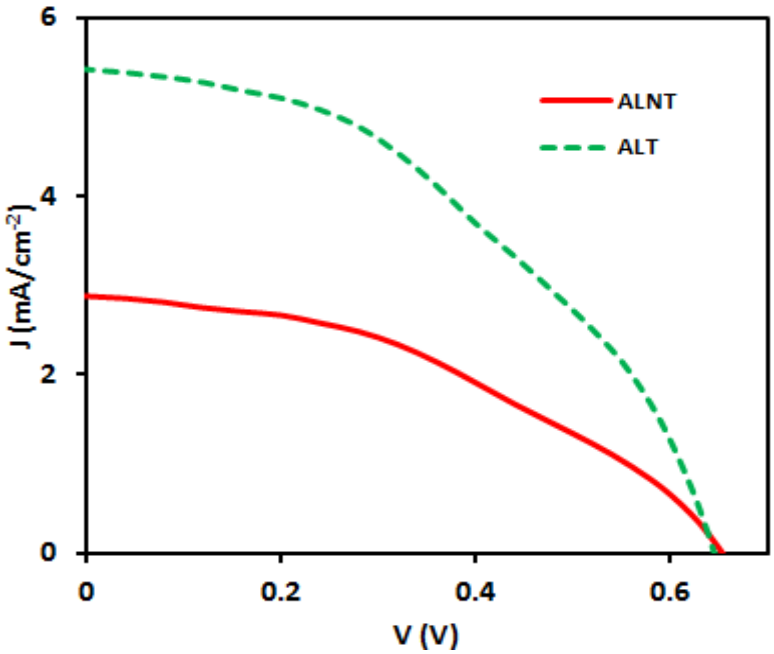

Figure 5. J-V curve for DSSCs based on ALT and ALNT nanoparticles as photoanode materials.

Table 1: The photovoltaic performance of ALT and ALNT photoanodes based DSSCs.

Sample	V_{OC} (V)	FF	J_{SC} (mA/cm^2)	Ƞ (%)
ALT	0.64	0.42	5.42	1.48
ALNT	0.65	0.41	2.88	0.77

The above value is relatively high as compared with the DSSC based on the ALNT sample i.e. current density (Jsc) 2.88 mA/cm^2 and efficiency (Ƞ) 0.77%. Al/N co-doped TiO_2 photoanode related DSSC. Table (1) summarizes the performance of the DSSCs.

Conclusion

Al-TiO_2 (ALT) and Al/N-TiO_2 (ALNT) nanoparticles were prepared by the sol-gel method and studied their performance. As compared to Al-TiO_2, Al/N-TiO_2 showed the wider diffraction peak as noticed by the XRD and Raman spectral studies. The broaden peak corresponds to the smaller crystallite size. FESEM morphological studies evidenced the preparation of the spherical nanoparticles while the presents of elemental peaks were confirmed by the EDS analysis. Furthermore, the prepared nanoparticles were employed for the preparation of DSSCs. The DSSC based on the Al-TiO_2 nanoparticles showed the enhanced short-circuit current (5.42 mA/cm^2) and efficiency (1.48%) as compared to the Al/N-TiO_2 based one. By optimizing the various properties of the synthesis the cell efficiency can be improved.

References

1. B. O'Regan, M. J. Gratzel. A low- cost, high- efficiency solar cell based on dye-sensitized colloidal TiO_2 films, *Nature*, 353(1991), 737–740. https://www.nature.com/articles/353737a0
2. S.J. Roh, R.S. Mane, S.K. Min, W.J. Lee, C.D. Lokhande, S.H. Hanb, Achievement of 4.51 % conversion efficiency using ZnO recombination barrier layer in TiO_2 based dye-sensitized solar cells, *Applied Physics Letters*, 89 (2006) 253512. https://www.nature.com/articles/353737a0.pdf
3. M.J. Gratzel, Dye-sensitized solar cell, *Journal of Photochemistry and Photobiology C: Photochemistry Reviews*, 4(2003), 145–153. https://doi.org/10.1016/S1389-5567(03)00026-1

4. K.S. Dhonde, M. Dhonde, V. V. S. Murthy, Novel synergistic combination of Al/N co-doped TiO_2 nanoparticles for highly efficient dye-sensitized solar cells, *Solar Energy*, 173(2018), 551-557. https://doi.org/10.1016/j.solener.2018.07.091
5. K. Kakiage, Y. Aoyama, T. Yano, K. Oya, Jun-ichi Fujisawa, M. Hanaya, Highly-efficient dye-sensitized solar cells with collaborative sensitization by silyl-anchor and carboxy-anchor dyes, *Chemical Communications*, 51(2015), 15894-15897. https://pubs.rsc.org/en/content/articlelanding/2015/cc/c5cc06759f#!divAbstract
6. R. Jose, V. Thavasi, S. Ramakrishna, Metal oxides for dye-sensitized solar cells, *Journal of the American Ceramic Society, 92* (2009), 289-301. https://doi.org/10.1111/j.1551-2916.2008.02870.x
7. E.M. Jin, S.M. Jeong, H.C. Kang, H.B. Gu, The photovoltaic effect of metal-doped TiO_2 nanoparticles for dye-sensitized solar cells, *ECS Journal of Solid State Science and Technology*, 5 (2016) Q109-Q114. http://jss.ecsdl.org/content/5/5/Q109.short
8. M.C. Wu, S.H. Chan, M.H. Jao, W.F. Su, Enhanced short-circuit current density of perovskite solar cells using Zn-doped TiO_2 as electron transport layer, *Solar Energy Materials & Solar Cells*, 157(2016), 447-453. https://doi.org/10.1016/j.solmat.2016.07.003
9. R. Li, Y. Zhao, R. Hou, X. Ren, S. Yuan, Y. Lou, Z. Wang, D. Li and L. Shi, Enhancement of power conversion efficiency of dye sensitized solar cells by modifying mesoporous TiO_2 photoanode with Al doped TiO_2 layer, *Journal of Photochemistry and Photobiology A: Chemistry*, 319-320(2016), 62-69. https://doi.org/10.1016/j.jphotochem.2016.01.002
10. R. Govindaraj, M. Senthil Pandian, P. Ramasamy, S. Mukhopadhyay, Sol-gel synthesized mesoporous anatase titanium dioxide nanoparticles for dye-sensitized solar cell (DSSC) applications, *Bulletin Materials Science*, 38(2015), 291-296.https://link.springer.com/article/10.1007/s12034-015-0874-3
11. K. Sahu and V.V. S. Murthy "Novel sol-gel method of synthesis of pure and aluminium-doped TiO_2 nanoparticles" *Indian Journal of Pure & Applied Physics*, 54(2016), 485-488. http://op.niscair.res.in/index.php/IJPAP/article/view/12333
12. K. Sahu Dhonde, M. Dhonde and V.V.S. Murthy "Novel synergistic combination of Al/N Co-doped TiO_2 Nanoparticles for highly efficient dye-sensitized solar cells" *Solar Energy*, 173(2018), 551-557. https://doi.org/10.1016/j.solener.2018.07.091
13. L. Shaoyou, Lu Jianping, Feng Qingge and T. Wenhua, Effect of ethanol on synthesis and electrochemical property of mesoporous Al-doped titanium dioxide via solid-state reaction, Chinese Journal of Chemical Engineering, 19(2011), 674-681. https://doi.org/10.1016/S1004-9541(11)60040-2
14. Y.Y. Gurkan, E. Kasapbasi, N. Turkten and Z. Cinar, Influence of Se/N Codoping on the structural, optical, electronic and photocatalytic properties of TiO_2, *Molecules*, 22(2017), 1-17. https://www.ncbi.nlm.nih.gov/pmc/articles/PMC6155415/
15. S. Liu, G. Liu, Q. Feng, Al-doped TiO_2 mesoporous materials synthesis and photodegradation properties, *Journal of Porous Materials*, 17(2010), 197-206. https://link.springer.com/article/10.1007/s10934-009-9281-8
16. X. Cheng, X. Yu, Z. Xing, L. Yang, Synthesis and Characterization of N-Doped TiO_2 and Its Enhanced Visible-Light Photocatalytic Activity, *Arabian Journal of Chemistry*, 9 (2016) S1706-S1711. https://doi.org/10.1016/j.egypro.2011.09.058
17. Desireé M. de Los Santos, Javier Navas, Antonio Sánchez-Coronilla, Rodrigo Alcántara, Concha Fernández-Lorenzo, Joaquín Martín-Calleja, Highly Al-doped TiO_2 nanoparticles produced by Ball Mill Method: structural and electronic characterization, *Materials Research Bulletin*, 70 (2015) 704-711. https://doi.org/10.1016/j.materresbull.2015.06.008